Published in final edited form as:

Nat Mater. 2014 June ; 13(6): 653–661. doi:10.1038/nmat3922.

Injectable and bioresponsive hydrogels for on-demand matrix metalloproteinase inhibition

Brendan P. Purcell[‡], **David Lobb**[+], **Manoj B. Charati**[‡], **Shauna M. Dorsey**[‡], **Ryan J. Wade**[‡], **Kia N. Zellers**[+], **Heather Doviak**[+], **Sara Pettaway**[+], **Christina B. Logdon**[+], **James Shuman**[+], **Parker D. Freels**[+], **Joseph H. Gorman**[#], **Robert C. Gorman**[#], **Francis G. Spinale**[+], and **Jason A. Burdick**[‡,*]

[‡]Department of Bioengineering, University of Pennsylvania, Philadelphia, PA

[+]Cardiovascular Translational Research Center, University of South Carolina School of Medicine and the WJB Dorn Veteran Affairs Medical Center, Columbia, SC

[#]Gorman Cardiovascular Research Laboratory, Department of Surgery, University of Pennsylvania, Philadelphia, PA

Abstract

Inhibitors of matrix metalloproteinases (MMPs) have been extensively explored to treat pathologies where excessive MMP activity contributes to adverse tissue remodeling. While MMP inhibition remains a relevant therapeutic target, MMP inhibitors have not translated to clinical application due to the dose-limiting side effects following systemic administration of the drugs. Here, we describe the synthesis of a polysaccharide-based hydrogel that can be locally injected into tissues and releases a recombinant tissue inhibitor of MMPs (rTIMP-3) in response to MMP activity. Specifically, rTIMP-3 is sequestered in the hydrogels through electrostatic interactions and is released as crosslinks are degraded by active MMPs. Targeted delivery of the hydrogel/rTIMP-3 construct to regions of MMP over-expression following a myocardial infarction (MI) significantly reduced MMP activity and attenuated adverse left ventricular remodeling in a porcine model of MI. Our findings demonstrate that local, on-demand MMP inhibition is achievable through the use of an injectable and bioresponsive hydrogel.

Excessive extracellular matrix (ECM) proteolysis by matrix metalloproteinases (MMPs) is a hallmark of many human disease states including chronic inflammation, tumor progression, and cardiovascular disease [1]. MMPs hydrolyze peptide bonds with a high level of amino acid specificity, and under normal physiological conditions MMP activity is precisely controlled - such as through tissue inhibitors of MMPs (TIMPs) - to maintain a low level of

[*]Corresponding Author: University of Pennsylvania, Department of Bioengineering, 240 Skirkanich Hall, 210 S. 33rd Street, Philadelphia, PA 19104; Tel: 215-898-8537; Fax: 215-573-2071; burdick2@seas.upenn.edu.

Author contributions. B.P.P, M.B.C, R.C.G., F.G.S., and J.A.B. conceived the ideas and designed the experiments. B.P.P., D.L., M.B.C., S.M.D., R.J.W., K.N.Z, H.D., S.P., C.B.L., J.S., and P.D. Freels conducted the experiments and analyzed the data. B.P.P., J.H.G., R.C.G, F.G.S., and J.A.B interpreted the data and wrote the manuscript.

Additional information. Supplementary information is available in the online version of the paper. Reprints and permissions information is available online at www.nature.com/reprints. Correspondence and requests for materials should be addressed to J.A.B.

structural protein, cell receptor, and growth factor turnover. However, under pathophysiological conditions, there is a persistence of MMP activity which causes maladaptive changes to tissue architectures and functions, contributing to disease progression [2]. Towards the development of therapies to treat this, the design and development of molecules that inhibit MMP activity has been a widely explored area of research over the past 25 years [1,3]; however, none have translated to clinical application due to the dose-limiting side effects following systemic administration of these pharmacological MMP inhibitors[4]. To limit off-target effects of therapeutics, biomaterials – including injectable and water-swollen polymer networks or hydrogels – have acted as depots to locally deliver therapeutics based on diffusion and degradation mechanisms [5-7]. Typically, these material systems are engineered to achieve a release profile to adequately dose patients within a therapeutic window specific to a disease. However, the absolute magnitude and temporal variation of MMP activity in patients is highly variable[8,9]; therefore, one hydrogel formulation and inhibitor dose may not be widely applicable across patient populations.

As an alternative to passive delivery, the recent development of stimuli responsive polymers have improved our ability to deliver therapeutics based on a trigger, such as light, pH, temperature, or the presence of an enzyme [10], including MMPs [11-16]. We present here the development of an MMP-degradable hydrogel that is both injectable and sequesters TIMPs through charge interactions, so that local MMP activity regulates the release of a recombinant TIMP. This approach has not been previously used; yet, it has implications in numerous applications where MMP dysregulation leads to disease progression and where heterogeneity in MMP levels makes uniform therapeutic dosing difficult.

One specific area where MMP induction is associated with disease progression is the adverse left ventricle (LV) remodeling in patients following a myocardial infarction (MI) [17,9]. Experimental models involving transgenic deletion of specific MMPs and systemic administration of pharmacologic MMP inhibitors have demonstrated that MMPs are important contributors to adverse global LV remodeling including LV wall thinning, chamber dilation, and ultimately dysfunction [18-21]. While systemic administration of pharmacologic MMP inhibitors has shown efficacy in attenuating post MI remodeling in pre-clinical animal models of MI[20,22], off-target effects have limited their success in recent clinical trials [23,24]. Further, recent studies have shown that MMP elevation is highly localized to ischemic tissue within the MI region following experimental MI in large animal models [25,26]. While MMP levels increased dramatically, levels of TIMPs decreased significantly within the MI region [26]. With the exception of TIMP-1, TIMPs are known to inhibit all of the 25 known MMPs, and studies have identified unique roles and functionalities of each of the four TIMPs [27]. Regarding TIMP-3, myocardial TIMP-3 levels were significantly reduced in contradistinction to elevated myocardial MMP levels in patients with end-stage heart failure [28] and transgenic TIMP-3 deletion in experimental animal models caused adverse LV remodeling and accelerated progression to heart failure following MI [29,30,31]. Therefore, strategies that localize TIMP-3 to regions of MMP overexpression and limit spill over into the systemic circulation could safely target post MI remodeling by restoring MMP/TIMP imbalance within the MI region.

Hydrogels that form upon injection into the myocardium have recently been developed and applied post MI [32-36]. Building on these advances, we designed an injectable hydrogel with MMP-degradable crosslinks to encapsulate a recombinant TIMP-3 and release the inhibitor in response to elevated MMP expression within the myocardium following MI. One challenge towards realizing on-demand TIMP-3 delivery is to minimize passive TIMP-3 release from the hydrogels (i.e., in the absence of MMP activity). TIMP-3 is unique among the TIMPs in that it is found bound to the ECM of tissues while the other three TIMPs are presented as soluble proteins [37]. Specifically, TIMP-3 binds to sulfated glyocosaminoglycans with a high affinity through an abundance of positively charged lysine and arginine residues exposed on the protein surface [38,39]. TIMP-3 binding to the ECM is thought to facilitate local MMP inhibition in tissues, and recent studies have shown that sulfated polymers enhance TIMP-3 binding affinity for specific MMPs [40]. Therefore, we developed injectable hydrogels with a negatively charged polysaccharide backbone to mimic native TIMP-3/ECM interactions and minimize passive diffusion of TIMP-3 from the hydrogels. MMP-cleavable crosslinks were incorporated to liberate bound TIMP-3 in the presence of local MMP activity. Further, we utilized conjugation and crosslinking chemistries to form hydrogels rapidly upon injection into the myocardium that are stable in the absence of MMP activity to further prevent the passive release of TIMP-3 from the injection site. We demonstrate that this TIMP-3 delivery strategy is responsive to elevated MMP activity post MI, and effectively inhibits MMP activity within the MI region without raising systemic TIMP-3 levels. Importantly, locally inhibiting MMP activity within the myocardium attenuated post MI remodeling as evidenced through significant improvements in LV geometry and function in a large animal model of MI.

Injectable and bioresponsive hydrogel design

The main criteria used in designing a hydrogel formulation for rTIMP-3 delivery were to 1) form hydrogels upon injection of macromolecules through a syringe, 2) have the hydrogels degrade only in the presence of MMPs, and 3) minimize passive release of encapsulated rTIMP-3 (i.e., in the absence of MMP activity). Towards this goal, we developed a three-macromer system that utilizes the chemical versatility of polysaccharide backbones (Fig. 1a). Polysaccharides were chemically modified to contain either aldehyde (ALD) or hydrazide (HYD) functional groups to form hydrogels in a one-step condensation reaction, with water as the only byproduct (Fig. 1b). Hyaluronic acid (HA) was used as a template for both ALD and HYD modifications due to the well-defined size ranges of commercially available HA, the previous use of HA in biomedical applications, and the abundance of diol and carboxylic acid groups necessary for ALD and HYD modifications, respectively [41]. Dextran sulfate (DS) was also incorporated into the hydrogels through ALD modification of its diol groups to act as a heparin mimetic to immobilize encapsulated heparin-binding TIMP-3 [42].

ALD modification of HA and DS were evaluated separately as each polysaccharide contains a different number of diol groups amendable to aldehyde modification (Fig. S1). Further, converting diols to aldehydes through periodate oxidation is known to degrade polysaccharides, so a large molecular weight (MW) HA (~350kDa) was chosen to provide sufficient HA-ald MW to allow formation of robust hydrogels for rTIMP-3 encapsulation.

Reaction conditions for HA-ald were chosen to balance aldehyde modification and macromer MW as periodate concentration both increased aldehyde modification and decreased HA MW in a dose-dependent manner (Fig. S2). Reaction conditions for DS-ald were chosen to provide sufficient aldehyde modification to crosslink DS-ald into the hydrogel.

MMP-sensitivity was incorporated into the hydrogels by generating the MMP-cleavable peptide GGRMSMPV with functional groups at both ends for chemical conjugations using solid phase peptide synthesis. The peptide was synthesized with a HYD group at the N terminus to react with ALD containing polymers for hydrogel crosslinking, and a thiol group at the C terminus through incorporation of a cysteine amino acid to facilitate thioether linkage to a maleimide functionalized HA (MAHA) in a one-step click reaction (Fig. 1a). Finally, to improve solubility for passage of the polymer solution through a syringe, hydrophilic serine (S) and asparagine (N) spacers were incorporated between the functional groups and the MMP-cleavable sequence. Successful synthesis of the designed peptide was verified with mass spectroscopy (Fig. S3) and peptide coupling to MAHA was verified by complete consumption of the characteristic maleimide peak from ^{1}H NMR (Fig. S4). The thioether coupling chemistry was chosen for its stability in water to prevent non-specific hydrolysis of the hydrogels.

The designed macromers rapidly formed hydrogels upon mixing ALD and HYD modified macromers over a range of macromer weight percents (1-5 wt%) as evidenced by development of the elastic component (G') of the complex modulus using rheometry (Fig. S5). The time to gelation and the ultimate modulus decreased and increases, respectively, with an increase in macromer concentrations. At 3.5 wt%, the hydrogels formed solid gels (G' > G'') in less than 1 minute and reached a final G' of approximately 1.5 kPa within 10 minutes, at which point the hydrogels were robust, nearly elastic solids (Fig. 1c). To demonstrate MMP-sensitivity, hydrogels were incubated in buffer with varying concentrations of active MMPs and uronic acid content in the buffer was measured over time to calculate hydrogel mass loss. In the absence of active MMPs, the 3.5 wt% hydrogels were stable over the 12-day study (Fig. 1d). However, with 20 U/mL enzyme concentration, the hydrogels degraded in a near-linear fashion with very little hydrogel remaining after 12 days, and with 200 U/mL, the hydrogels completely degraded in 2 days. In addition to enzyme concentration, hydrogel degradation rate was also controlled by macromer concentration (Fig S6). Hydrogel degradation rates scaled inversely with macromer concentration and therefore the number of crosslinks in the hydrogel. To evaluate the applicability of the hydrogels for MMP-triggered release of encapsulated molecules, FITC-BSA was encapsulated in 3.5 wt% hydrogels and release was quantified in buffer with varying concentrations of active MMPs. Encapsulated FITC-BSA release followed the hydrogel degradation behavior in a similar MMP-dependent manner (Fig. 1e).

MMP triggered rTIMP-3 release

TIMP-3 was chosen for local delivery post-MI in part because of its unique ECM-binding property. This allowed us to design ECM mimetic hydrogels to encapsulate and bind rTIMP-3 until released by MMP-mediated hydrogel degradation. To this end, DS was

incorporated into the hydrogel formulation to mimic sulfated GAGs, the major component of the ECM responsible for TIMP-3 binding, due to its susceptibility to aldehyde modification through diol oxidation. Binding of rTIMP-3 to DS-ald was evaluated using a solid-phase binding assay. rTIMP-3 bound to DS-ald with a much greater capacity than to HA-ald, and approached the capacity of rTIMP-3 binding to heparin (Fig. 2a). Importantly, rTIMP-3 binding to DS-ald did not reduce rTIMP-3 inhibition of active MMPs (Fig. 2b). rTIMP-3 inhibited 4nM rMMP-2 with a half maximal inhibitory concentration of 17±4 ng/mL (0.7±0.2 nM) with 50 μg/mL DS-ald in solution compared to 28±7 ng/mL (1.2±0.3 nM) without DS-ald in solution ($p=0.07$). Previous studies found that a stretch of basic amino acids responsible for TIMP-3 binding to sulfated GAGs is opposite to the TIMP-3 reactive site that interacts with MMPs [39]. Therefore, utilizing polysaccharides that mimic sulfated GAGs allows localization of TIMP-3 without altering its inhibitory properties. Indeed, incorporating the sulfated DS-ald polymers into the hydrogels drastically reduced passive release (from ~95 to 20%) of encapsulated rTIMP-3 over the 14 day study, allowing for MMP-triggered release of the rTIMP-3 remaining in the hydrogel over a range of MMP activities and durations (Fig. 2c). In addition, increasing the weight percent of the macromers beyond 3.5 wt% did not further reduce passive rTIMP-3 diffusion from the hydrogel (Fig S7).

To investigate the responsiveness of the rTIMP-3 containing hydrogels to MMP-2 activity, hydrogels with and without encapsulated rTIMP-3 were incubated in 20 nM active rMMP-2. MMP-2 is ubiquitously expressed in all tissue types, is robustly upregulated in pathological remodeling, and degrades common ECM structural proteins. Thus, recombinant MMP-2 was utilized as the “prototypical MMP” for the purposes of *in vitro* validation studies. Hydrogels without rTIMP-3 degraded within 2 days in the MMP buffer, while hydrogels with encapsulated rTIMP-3 degraded in a linear fashion for over 14 days (Fig. 2d). This reduction in hydrogel degradation rate observed with rTIMP-3 encapsulation indicates that encapsulated rTIMP-3 remains active and is inhibiting rMMP-2 activity as rMMP-2 is degrading the hydrogel (Fig. 2e). Further, since rMMP-2 was refreshed every 2 days to account for enzyme stability (Fig. S8), a sufficient amount of active rTIMP-3 remained bound in the hydrogel for the entire 14 day study, otherwise the hydrogel would rapidly degrade in similar fashion to the hydrogels without rTIMP-3. These results demonstrate a novel approach of locally delivering rTIMP-3 in response to MMP activity by designing injectable hydrogels containing MMP-cleavable crosslinks and sulfated GAGs, where the local presence of active MMPs controls the release of matrix-bound rTIMP-3, and therefore local MMP inhibition.

Hydrogel formation and degradation *in vivo*

To assess the effectiveness of our rTIMP-3 delivery system in the setting of pathological MMP overexpression, a large animal model of MI was employed that allows for regional quantification of MMP expression and activity, along with functional outcomes of post MI LV remodeling [20,21]. Hydrogels with encapsulated rTIMP-3 were injected at 9 equally spaced sites (100 μL of hydrogel per injection site) within a 2 cm × 2 cm grid in the ischemic, MI region of the myocardium (Fig. 3a). A dual-barreled syringe was utilized to

blend ALD and HYD polymers in equal ratios immediately prior to entering the tissue for *in situ* crosslinking.

Hydrogels were first injected into myocardium with either elevated MMP activity (MI myocardium) or normal MMP activity (non-MI myocardium) and hearts were harvested after 0 or 14 days to evaluate hydrogel crosslinking and degradation in response to MMP activity. Using a magnetic resonance imaging (MRI) technique to visualize hydrogels in the myocardium [43], dense regions of hydrogel were observed throughout the myocardial wall immediately after injection (Fig. S9). The hydrogel chemical composition produces a higher MR signal compared to myocardial tissue, resulting in brighter regions on the MRI image. Three-dimensional reconstruction of the hydrogel from the MRI images indicates that the hydrogels formed pockets as they were injected into the myocardium, and some extravasated (~10 μL per injection) back along the needle track as the hydrogel crosslinked from a liquid into a solid (Fig. 3b). The presence of solid hydrogel pockets was confirmed with histology as the negatively charged hydrogel stained dark purple with hematoxylin and eosin staining (Fig. 3c). The presence of the hydrogels was also confirmed with hyaluronidase treatment of the tissue sections, as HA is the major component of the hydrogels (Fig S10).

After 14 days *in vivo* in myocardium with a normal, low level of MMP activity (sham instrumented pigs), pockets of hydrogel were still visible with MRI (Fig. 3c). Some regions of hydrogel appeared to be remodeled with infiltrating cells and tissue. In contrast, 14 days following injection into hearts with pathological levels of MMP activity (MI instrumented pigs), pockets of hydrogel were no longer visible with MRI or histology (Fig. 3c-d). Instead, a more disperse signal from the scar tissue was visible with MRI and very little remnants of hydrogel was observed with histology. Quantification of the hydrogels with histology showed a drastic and significant reduction of hydrogel in MI hearts after 14 days *in vivo* compared to day 0 (Fig. 3e). In addition, there was significantly less hydrogel in the MI hearts compared to sham hearts after 14 days *in vivo* (Fig. 3e). This indicates that hydrogel degradation was responsive to increased MMP activity in infarct tissue following MI compared to normal tissue, and therefore the injected hydrogel released encapsulated rTIMP-3 in proportion to MMP activity within the tissue. This is an important observation as MMP expression varies both spatially and temporally from patient to patient post MI[8,9], and therefore bioresponsive constructs such as this one could be used to release MMP inhibitors based on local MMP triggers instead of relying on a “one-size fits all” approach to inhibitor dosing.

Therapeutic efficacy post MI

Next, to assess the biological effects of this bioresponsive delivery system post MI, hydrogels containing rTIMP-3 were injected immediately following MI and 14-day outcomes were compared to sham controls, MI only, and MI with hydrogel only injection. Endogenous TIMP-3 concentrations in the MI region were restored to normal non-MI levels 14 days following MI induction and hydrogel/rTIMP-3 injections (Fig. 4a). To assess systemic spillover of delivered rTIMP-3, blood samples were taken after 1, 3, 7, and 14 days following myocardial injections and analyzed for TIMP-3 concentrations. Importantly, there was no observed increase in systemic TIMP-3 levels with hydrogel delivery of rTIMP-3 to

the MI region compared to control groups (Fig. 4b). Together, these TIMP-3 analyses confirm local delivery of rTIMP-3 to the myocardium while limiting spillover into the circulation. To quantify the effects of locally delivered rTIMP-3 on MMP activity, interstitial MMP activity within the MI region was quantified *in vivo* using a previously validated microdialysis technique [8]. Using this technique, interstitial MMP activity was observed to significantly increase in the MI region 14 days following MI induction (Fig. 4c). Interestingly, injection of the MMP degradable hydrogels alone significantly reduced interstitial MMP activity within the MI region, due to the peptide crosslinks in the hydrogel being cleaved by MMPs, reducing substrate hydrolysis elsewhere. However, rTIMP-3 delivery from the MMP degradable hydrogels further reduced interstitial MMP activity within the MI region. To further quantify MMP activity, myocardial extracts isolated 14 days post MI were digested and subjected to MMP activity assays *in vitro*[22]. Substrates for both global MMP activity and membrane type-1 (MT1-MMP) specific activity, an important activator of other MMPs[2], were significantly increased in the MI region in the MI only and MI/hydrogel injection groups; however, there was no significant increase in global or MT1-MMP activity in the MI region following rTIMP-3 delivery from the hydrogels (Fig. 4d). MMP activity levels in remote myocardium (non-MI region) showed no change from normal levels following MI or hydrogel treatment. Gene expression of MMPs 14 days following MI and hydrogel treatments showed a significant reduction in the expression of membrane type MMPs (MMP-14) with hydrogel and hydrogel/rTIMP-3 injections, while only hydrogel/rTIMP-3 injections showed a significant reduction in collagenase (MMP-13) expression compared to MI and hydrogel injection alone (Fig. S11). MMP-13 is expressed at very low levels in normal tissue such as myocardium, but is robustly expressed in both animal models and humans with heart failure [26,44]. The expression and activation of MMP-13 is considered to be associated with pathological remodeling processes [45], and thus the reduction in this MMP type with hydrogel/rTIMP-3 injections holds relevance. In addition, MMP expression was not altered compared to sham in remote myocardium following hydrogel/rTIMP-3 treatment (Fig. S11).

To assess myocardial tissue structure, tissue sections were stained for collagen content and α-smooth muscle actin (SMA) (Fig. S12). There was a significant increase in collagen content following MI in all groups, and no significant effect of hydrogel or hydrogel/rTIMP-3 delivery on collagen content. This is an important observation as increased collagen content induced by rTIMP-3 delivery would suggest acceleration of fibrosis, rather than a stabilization of the matrix within the MI region. Further, there was a significant increase in SMA content in all groups following MI indicating the typical transdifferentiation of fibroblasts to myofibroblasts[46], and no significant effect of hydrogel or hydrogel/rTIMP-3 delivery on SMA content. In addition, there were comparable gene expression levels of fibronectin variant, extra domain-1 (EDA) across all groups 14 days following MI indicating a consistent myofibroblast transdifferentiation within the MI region (Fig. S13) [47,48]; however, there was only a significant increase in the gene expression of a myosin heavy chain isoform (MYH14) in the hydrogel/rTIMP-3 group. As MYH14 is associated with a more mature, contractile myofibroblast [47,48], rTIMP-3 delivery appears to have driven fibroblast transdifferentiation to a more contractile phenotype, over and above that of MI and hydrogel injection alone.

To assess the effects of rTIMP-3 delivery on global LV remodeling, serial echocardiographic measurements were made for 14 days following experimental MI induction in all groups (Fig 5a). MI induction caused a gradual reduction in LV function, as indicated by a declining ejection fraction (EF) and a progressive increase in chamber dilation (left ventricular end-diastolic volume, LVEDV) and MI thinning - all key events in the progression of adverse post MI remodeling (Fig. 5a-c). A pathophysiological determinant of worsening LV function and progression to heart failure post MI, is an increase in pulmonary capillary wedge pressure (PCWP)[17], and indeed this index increased in a time dependent manner post MI (Fig. 5d). With the injection of the MMP sensitive hydrogels and rTIMP-3 release, LV EF was improved, chamber dilation reduced, MI thickness increased and the progressive increase in PCWP attenuated. Thus, during this early and critical time point of post MI remodeling (14 days), a significant beneficial effect on LV function and geometry was demonstrated with the hydrogel and TIMP-3 delivery when compared to appropriate control systems. Further, echocardiographic assessment of another group of pigs was performed out to 28 days and showed that the therapeutic benefit of hydrogel/rTIMP-3 injections was maintained (Fig. 5f, S1). Significantly attenuating LV wall thinning and dilation to this time point is expected to have a significant lasting benefit on LV function as the fastest rate of LV dilation occurs in patients within the first 28 days post MI [9].

Collectively, these results demonstrate the utility of injectable and bioresponsive hydrogels to locally deliver TIMPs in response to excessive MMP activity. This is the first proof-of-concept demonstration of designing MMP-degradable hydrogels to release an MMP inhibitor in the presence of MMP activity to limit off-target effects of MMP inhibitors, which have been clinically problematic, and to provide on-demand presentation of an inhibitor based on local MMP activity. The successful demonstration of this technology in attenuating post MI remodeling in a large animal model warrants further pre-clinical investigation as it could ultimately provide a safe and effective therapy to treat patients in the clinical setting of acute MI. Ultimately, this strategy can be used for any disease where the local imbalance of MMPs and their inhibitors leads to disease progression.

Methods

Solid-phase peptide synthesis

Peptides were synthesized with the MMP-cleavable sequence GCNSGGRMSMPVSNGG-Hyd where C is the cysteine containing a thiol group that was used for coupling to a maleimide functionalized HA and Hyd is the hydrazide for hydrogel crosslinking with an aldehyde functionalized HA (see Supplemental Methods).

Synthesis and characterization of polymers

HA-peptide-hydrazide polymers were synthesized by coupling a cysteine terminated peptide to HA-maleimide (see Supplemental Methods) by mixing in a 4:1 molar ratio, cysteine:maleimide in PBS for 4hrs at 4°C. The polymer was purified by dialysis against a 20 mM NaCl solution for 5 days and then DI water for 3 days, frozen and lyophilized. HA-aldehyde was synthesized by mixing NaHy (350kDa, Lifecore) at 1 % (w/v) and sodium

periodate (IO_4) in DI water at a molar ratio of 1:2 HA:IO_4 for 2hrs at RT. The reaction was stopped by adding 10% (v/v) ethylene glycol to the reaction, dialyzing against DI water for 5 days, freezing and lyophilizing. DS-ald was synthesized in a similar fashion except DS (Sigma) was reacted with IO_4 at a molar ratio of 2:1 DS:IO_4 for 5hrs at RT. Percent aldehyde modification was quantified using a TNBS colorimetric assay as previously described [49].

Rheometry

To form 3.5 wt% hydrogels, ALD (2.4% HA-ald, 1.4% DS-ald (w/v)) and HYD (3.2% (w/v) HA-MMP-hyd) modified polymers were dissolved in PBS, mixed 1:1 (v/v) for 1:1 ALD:HYD and gelation characteristics were quantified by monitoring the storage (G') and loss (G'') moduli with time using an AR2000ex Rheometer (TA Instruments) at 37°C under 1% strain and 1 Hz.

Hydrogel degradation and molecule release studies

FITC-BSA or rTIMP-3 was mixed with the ALD precursor solution and hydrogels were formed as described above in cylindrical molds for 30 min at 37°C. Hydrogels were incubated in PBS supplemented with 1% BSA for FITC-BSA studies or TTC buffer (50mM Tris-HCl, 1mM $CaCl_2$, 0.05% triton x-100, pH 7.5) for rTIMP-3 studies at 37°C. Enzymes (collagenase type 4, Worthington or rMMP-2, R&D Systems) were added every 2 days and buffers were collected and stored at −20°C prior to analysis. Uronic acid content was analyzed to calculate hydrogel mass loss [33], FITC-BSA fluorescence was analyzed to measure release, and an ELISA was used to measure rTIMP-3 content (R&D Systems).

rTIMP-3 activity and binding assays

rTIMP-3-His (Amgen, Inc.) activity was quantified by its ability to inhibit rMMP-2 (R&D Systems) activity using an MMP cleavable fluorogenic substrate (R&D Systems). Serial dilutions of rTIMP-3 were added to 4 nM activated rMMP-2 in TTC buffer, incubated for 2 hrs at 37°C, then the fluorogenic substrate was added and fluorescence kinetics were measured over 5 min with a microplate reader (Tecan). rTIMP-3 binding to polysaccharide polymers was evaluated with a solid-phase binding assay (See Supplemental Methods).

MI induction and hydrogel injections

Yorkshire pigs (n=43, 25kg, Hambone Farms, Orangeburg, SC) were anesthetized with isoflurane (2%) and the LV free wall was exposed through a left thoracotomy. All animals were treated and cared for in accordance with the National Institutes of Health Guide for the Care and Use of Laboratory Animals, and all protocols were approved by the University of South Carolina's Institutional Animal Care and Use Committee. A square calibrated grid was sutured below the origin of the first two obtuse marginal arteries of the circumflex artery (OM1 and OM2), which provided for a total of 9 distinct injection sites within a targeted 2×2 cm region of myocardium (Fig. 3a). OM1 and OM2 were ligated to induce an MI, and characteristic ECG changes occurred, but electrical cardioversion and/or defibrillation were not required. Past studies demonstrated that this technique creates a uniform and consistent MI [20]. Sham controls were instrumented in a similar fashion with the

exception of coronary artery ligation. In addition, vascular access catheter placed in the descending aorta and connected to a subcutaneous port (6 Fr., SlimPort, Bard Access Systems, Salt Lake City). Pigs were randomized to receive injections of saline, hydrogel alone, or hydrogel with rTIMP-3 immediately following MI induction. For hydrogel injections, the ALD (2.4% HA-ald, 1.4% DS-ald (w/v)) and HYD (3.2% (w/v) precursors solutions were mixed in a sterile fashion, drawn into separate 1mL syringes, and injected into the mid-myocardium of each target site using a FibriJet blending connector (Nordson Micromedics, SA-3670) with a 27G needle. Hydrogels were injected immediately following MI induction. For the MI/hydrogel/rTIMP-3 group, rTIMP-3 was mixed into the ALD precursor (20μg rTIMP-3/100μL ALD). Successful injections were confirmed by visualization of an opacification of the epicardial surface at the point of myocardial injection.

Blood analysis

Blood samples (5 mL) were collected from the subcutaneous port 1, 3, 7 and 14 days post MI. The collected blood samples were centrifuged and the decanted plasma subjected to ELISA for TIMP-3.

LV assessment with echocardiography

Animals were sedated (20 mg valium, PO, Elkin-Sinn) and two-dimensional echocardiographic studies (GE VIVID 7 Dimension Ultrasound System: M4S 1.5-4.3 MHz active matrix array sector transducer probe) were performed to calculate LV dimensions and ejection fraction. Echocardiography measurements were taken 1 day prior to MI induction, and then again 1, 3, 7 and 14 days following MI in a subset of animals (n=27), and 3, 7, 14 and 28 days following MI in another subset of animals (n=9).

Interstitial MMP activity

After 14 days post MI, the pigs were anesthetized with sufentanyl (2μg/kg IV, Baxter Healthcare), morphine sulfate (3mg/kg/h IV, Elkin-Sinn), and isoflurane (1%, 3 L/min O_2, Baxter Healthcare), and mechanically ventilated. The LV was exposed through a sternotomy, a microdialysis probe (20 kDa, outer diameter of probe shaft 0.77mm; CMA/Microdialysis, North Chelmsford, MA) placed within the MI region, and infused with the MMP fluorescent substrate (5 μL/min) as previously validated [8,9]. The dialysate was then subjected to fluorometry, which reflected interstitial MMP activity, and these values were normalized to referent control values and expressed as a percent. Following these measurements, the LV was harvested, separated into MI and remote regions (area served by left anterior descending artery), and prepared for biochemical analysis.

Myocardial biochemical analysis

Immunoblotting was performed for total myocardial TIMP-3 using approaches described previously [20] (See Supplemental Methods). To determine ex-vivo MMP activity, LV myocardial extracts (50 μg) were incubated with the global MMP substrate described in the previous section. The steady-state maximal fluorescence units (FU) were recorded and all

assays were performed in triplicate. Expression of key determinants of ECM remodeling were analyzed via PCR (see Supplemental Methods).

MRI analysis

Full thickness LV myocardial sections were cut from cardiac explants around the 2 cm hydrogel injection grid and imaged on a 9.4T MRI Scanner (Siemens). A T2 weighted spin echo pulse sequence was employed with the following imaging parameters: echo time (TE) = 40 ms, repetition time (TR) = 4000 ms, averages = 4, matrix size = 256 × 256 × 88, field of view = 35 × 35 mm^2, voxel size = 0.14 × 0. 14 × 0.25 mm^3. MRI images were converted into NIFTI files using ImageJ software and imported into ITK-SNAP segmentation software as a stack of 2D images. 3D reconstructions of the hydrogel was performed using an automated segmentation algorithm in ITK-SNAP[50]. Briefly, the images were contrasted and hydrogel pockets were seeded for the algorithm (Fig. S9). Presence of the hydrogel was confirmed with histology (see Supplemental Methods).

Data and statistical analysis

Statistical analyses were performed using STATA statistical software (See Supplemental Methods).

Supplementary Material

Refer to Web version on PubMed Central for supplementary material.

Acknowledgements

The authors would like to thank Dr. TaeWeon Lee from Amgen, Inc for supplying the rTIMP-3 peptide used in this study, Dr. Weixia Liu, Dr. Stephen Pickup and Dr. Walter Witschey from Penn Medicine for MRI technical assistance expertise. This work was supported by funding from the National Institutes of Health (R01 HL107938, HL111090, HL095608,T32 HL007954), and a Veterans' Affairs Health Administration Merit Award (5101BX000168-03) to Dr. Francis Spinale.

References

1. Fingleton B. Matrix metalloproteinases as valid clinical targets. Curr Pharm Des. 2007; 13:333–346. [PubMed: 17313364]
2. Visse R, Nagase H. Matrix metalloproteinases and tissue inhibitors of metalloproteinases: structure, function, and biochemistry. Circ Res. 2003; 92:827–839. [PubMed: 12730128]
3. Abbenante G, Fairlie DP. Protease inhibitors in the clinic. Med Chem. 2005; 1:71–104. [PubMed: 16789888]
4. Turk B. Targeting proteases: successes, failures and future prospects. Nat Rev Drug Discov. 2006; 5:785–799. [PubMed: 16955069]
5. Hao XJ, et al. Angiogenic effects of sequential release of VEGF-A(165) and PDGF-BB with alginate hydrogels after myocardial infarction. Cardiovascular Research. 2007; 75:178–185. [PubMed: 17481597]
6. Ruvinov E, Leor J, Cohen S. The promotion of myocardial repair by the sequential delivery of IGF-1 and HGF from an injectable alginate biomaterial in a model of acute myocardial infarction. Biomaterials. 2011; 32:565–578. [PubMed: 20889201]
7. Peppas NA, Bures P, Leobandung W, Ichikawa H. Hydrogels in pharmaceutical formulations. European Journal of Pharmaceutics and Biopharmaceutics. 2000; 50:27–46. [PubMed: 10840191]

8. Spinale FG, Koval CN, Deschamps AM, Stroud RE, Ikonomidis JS. Dynamic changes in matrix metalloprotienase activity within the human myocardial interstitium during myocardial arrest and reperfusion. Circulation. 2008; 118:S16–23. [PubMed: 18824748]
9. Webb CS, et al. Specific temporal profile of matrix metalloproteinase release occurs in patients after myocardial infarction: relation to left ventricular remodeling. Circulation. 2006; 114:1020–1027. [PubMed: 16923753]
10. Stuart MAC, et al. Emerging applications of stimuli-responsive polymer materials. Nature Materials. 2010; 9:101–113. [PubMed: 20094081]
11. Lutolf MP, et al. Synthetic matrix metalloproteinase-sensitive hydrogels for the conduction of tissue regeneration: Engineering cell-invasion characteristics. Proceedings of the National Academy of Sciences of the United States of America. 2003; 100:5413–5418. [PubMed: 12686696]
12. Burdick JA, Murphy WL. Moving from static to dynamic complexity in hydrogel design. Nature Communications. 2012; 3
13. Phelps EA, Landazuri N, Thule PM, Taylor WR, Garcia AJ. Bioartificial matrices for therapeutic vascularization. Proceedings of the National Academy of Sciences of the United States of America. 2010; 107:3323–3328. [PubMed: 20080569]
14. Kim S, Healy KE. Synthesis and characterization of injectable poly(N-isopropylacrylamide-co-acrylic acid) hydrogels with proteolytically degradable cross-links. Biomacromolecules. 2003; 4:1214–1223. [PubMed: 12959586]
15. West JL, Hubbell JA. Polymeric biomaterials with degradation sites for proteases involved in cell migration. Macromolecules. 1999; 32:241–244.
16. Lutolf MP, et al. Repair of bone defects using synthetic mimetics of collagenous extracellular matrices. Nat Biotechnol. 2003; 21:513–518. [PubMed: 12704396]
17. Spinale FG, Zile MR. Integrating the myocardial matrix into heart failure recognition and management. Circ Res. 2013; 113:725–738. [PubMed: 23989715]
18. Ducharme A, et al. Targeted deletion of matrix metalloproteinase-9 attenuates left ventricular enlargement and collagen accumulation after experimental myocardial infarction. J Clin Invest. 2000; 106:55–62. [PubMed: 10880048]
19. Rohde LE, et al. Matrix metalloproteinase inhibition attenuates early left ventricular enlargement after experimental myocardial infarction in mice. Circulation. 1999; 99:3063–3070. [PubMed: 10368126]
20. Mukherjee R, et al. Myocardial infarct expansion and matrix metalloproteinase inhibition. Circulation. 2003; 107:618–625. [PubMed: 12566376]
21. King MK, et al. Selective matrix metalloproteinase inhibition with developing heart failure: effects on left ventricular function and structure. Circ Res. 2003; 92:177–185. [PubMed: 12574145]
22. Spinale FG, et al. Cardiac-restricted overexpression of membrane type-1 matrix metalloproteinase in mice: effects on myocardial remodeling with aging. Circ Heart Fail. 2009; 2:351–360. [PubMed: 19808359]
23. Peterson JT. The importance of estimating the therapeutic index in the development of matrix metalloproteinase inhibitors. Cardiovasc Res. 2006; 69:677–687. [PubMed: 16413004]
24. Overall CM, Kleifeld O. Tumour microenvironment - opinion: validating matrix metalloproteinases as drug targets and anti-targets for cancer therapy. Nat Rev Cancer. 2006; 6:227–239. [PubMed: 16498445]
25. Sahul ZH, et al. Targeted imaging of the spatial and temporal variation of matrix metalloproteinase activity in a porcine model of postinfarct remodeling: relationship to myocardial dysfunction. Circ Cardiovasc Imaging. 2011; 4:381–391. [PubMed: 21505092]
26. Wilson EM, et al. Region- and type-specific induction of matrix metalloproteinases in post-myocardial infarction remodeling. Circulation. 2003; 107:2857–2863. [PubMed: 12771000]
27. Brew K, Nagase H. The tissue inhibitors of metalloproteinases (TIMPs): an ancient family with structural and functional diversity. Biochim Biophys Acta. 2010; 1803:55–71. [PubMed: 20080133]
28. Fedak PW, et al. Matrix remodeling in experimental and human heart failure: a possible regulatory role for TIMP-3. Am J Physiol Heart Circ Physiol. 2003; 284:H626–634. [PubMed: 12388270]

29. Fedak PW, et al. TIMP-3 deficiency leads to dilated cardiomyopathy. Circulation. 2004; 110:2401–2409. [PubMed: 15262835]
30. Tian H, et al. TIMP-3 deficiency accelerates cardiac remodeling after myocardial infarction. J Mol Cell Cardiol. 2007; 43:733–743. [PubMed: 17945252]
31. Kassiri Z, et al. Simultaneous transforming growth factor beta-tumor necrosis factor activation and cross-talk cause aberrant remodeling response and myocardial fibrosis in Timp3-deficient heart. J Biol Chem. 2009; 284:29893–29904. [PubMed: 19625257]
32. Seif-Naraghi SB, et al. Safety and Efficacy of an Injectable Extracellular Matrix Hydrogel for Treating Myocardial Infarction. Science Translational Medicine. 2013; 5
33. Wall ST, Yeh CC, Tu RYK, Mann MJ, Healy KE. Biomimetic matrices for myocardial stabilization and stem cell transplantation. Journal of Biomedical Materials Research Part A. 95A2010:1055–1066.
34. Ifkovits JL, et al. Injectable hydrogel properties influence infarct expansion and extent of postinfarction left ventricular remodeling in an ovine model. Proc Natl Acad Sci U S A. 2010; 107:11507–11512. [PubMed: 20534527]
35. Segers VF, et al. Local delivery of protease-resistant stromal cell derived factor-1 for stem cell recruitment after myocardial infarction. Circulation. 2007; 116:1683–1692. [PubMed: 17875967]
36. Nelson DM, Ma ZW, Leeson CE, Wagner WR. Extended and sequential delivery of protein from injectable thermoresponsive hydrogels. Journal of Biomedical Materials Research Part A. 2012; 100A:776–785. [PubMed: 22237975]
37. Leco KJ, Khokha R, Pavloff N, Hawkes SP, Edwards DR. Tissue inhibitor of metalloproteinases-3 (TIMP-3) is an extracellular matrix-associated protein with a distinctive pattern of expression in mouse cells and tissues. J Biol Chem. 1994; 269:9352–9360. [PubMed: 8132674]
38. Yu WH, Yu S, Meng Q, Brew K, Woessner JF Jr. TIMP-3 binds to sulfated glycosaminoglycans of the extracellular matrix. J Biol Chem. 2000; 275:31226–31232. [PubMed: 10900194]
39. Lee MH, Atkinson S, Murphy G. Identification of the extracellular matrix (ECM) binding motifs of tissue inhibitor of metalloproteinases (TIMP)-3 and effective transfer to TIMP-1. J Biol Chem. 2007; 282:6887–6898. [PubMed: 17202148]
40. Troeberg L, et al. Pentosan polysulfate increases affinity between ADAMTS-5 and TIMP-3 through formation of an electrostatically driven trimolecular complex. Biochem J. 2012; 443:307–315. [PubMed: 22299597]
41. Burdick JA, Prestwich GD. Hyaluronic Acid Hydrogels for Biomedical Applications. Advanced Materials. 2011; 23:H41–H56. [PubMed: 21394792]
42. Huang M, Vitharana SN, Peek LJ, Coop T, Berkland C. Polyelectrolyte complexes stabilize and controllably release vascular endothelial growth factor. Biomacromolecules. 2007; 8:1607–1614. [PubMed: 17428030]
43. Kichula ET, et al. Experimental and Computational Investigation of Altered Mechanical Properties in Myocardium after Hydrogel Injection. Ann Biomed Eng. 2013
44. Spinale FG, et al. A matrix metalloproteinase induction/activation system exists in the human left ventricular myocardium and is upregulated in heart failure. Circulation. 2000; 102:1944–1949. [PubMed: 11034943]
45. Troeberg L, Nagase H. Proteases involved in cartilage matrix degradation in osteoarthritis. Biochim Biophys Acta. 2012; 1824:133–145. [PubMed: 21777704]
46. Zeisberg EM, et al. Endothelial-to-mesenchymal transition contributes to cardiac fibrosis. Nat Med. 2007; 13:952–961. [PubMed: 17660828]
47. Tomasek JJ, Gabbiani G, Hinz B, Chaponnier C, Brown RA. Myofibroblasts and mechano-regulation of connective tissue remodelling. Nat Rev Mol Cell Biol. 2002; 3:349–363. [PubMed: 11988769]
48. Goldsmith EC, Bradshaw AD, Spinale FG. Cellular mechanisms of tissue fibrosis. 2. Contributory pathways leading to myocardial fibrosis: moving beyond collagen expression. Am J Physiol Cell Physiol. 2012; 304:C393–402. [PubMed: 23174564]
49. Su WY, Chen YC, Lin FH. Injectable oxidized hyaluronic acid/adipic acid dihydrazide hydrogel for nucleus pulposus regeneration. Acta Biomater. 2010; 6:3044–3055. [PubMed: 20193782]

50. Yushkevich PA, et al. User-guided 3D active contour segmentation of anatomical structures: significantly improved efficiency and reliability. Neuroimage. 2006; 31:1116–1128. [PubMed: 16545965]

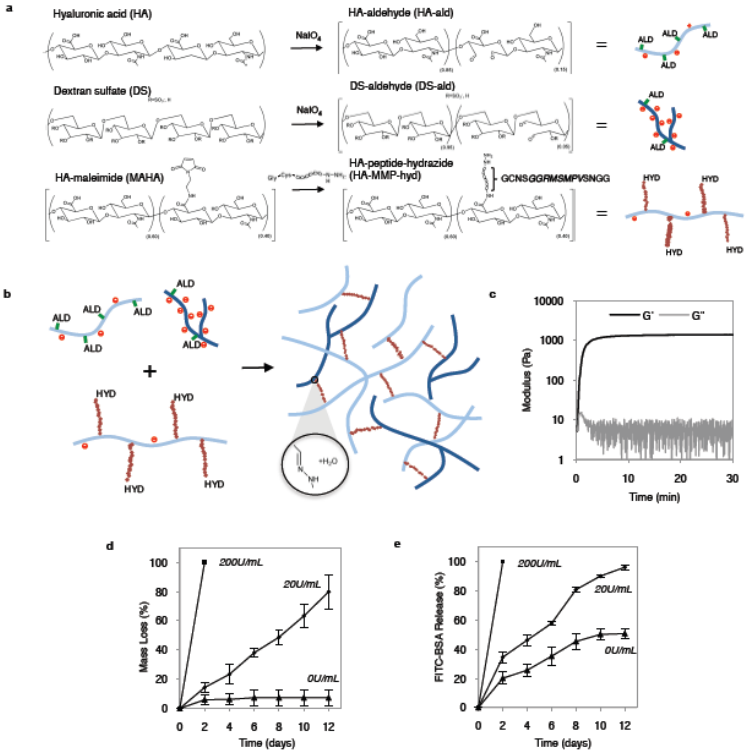

Figure 1. The fabrication of injectable and MMP-sensitive hydrogels for therapeutic delivery

(a) Hyaluronic acid (HA) and dextran sulfate (DS) polymers were modified with aldehyde (ALD) groups through periodate oxidation of diols along the polysaccharide backbone. ALD modifications for HA and DS were ~15% and 5% of the repeat disaccharides, respectively. A separate HA batch was modified with complimentary hydrazide (HYD) groups through conjugation of the peptide GCNS*GGRMSMPV*SNGG-hyd where C is a thiol containing cysteine to couple to a maleimide functionalized HA through a thiol-maleimide click reaction, hyd is the terminal hydrazide for hydrogel crosslinking, NS are hydrophilic spacers, and *GGRMSMPV* is the MMP-cleavable sequence. (b) Hydrogel crosslinking was designed through hydrazone bond formation of complimentary ALD and HYD groups to form hydrogels under physiologic conditions. (c) Upon mixing ALD (2.4 wt% HA-ald, 1.4 wt% DS-ald) and HYD (3.2 wt% HA-MMP-hyd) polymers, robust hydrogels formed rapidly as evidenced by development of storage (G') and loss (G'') moduli within minutes. (d-e) 3.5 wt% hydrogels were incubated with or without active MMPs (collagenase type 4). MMPs were refreshed every 2 days to maintain enzyme activity throughout the study. (d) Hydrogels were stable in the absence of enzyme activity (0 U/mL) and degraded in response to increasing enzyme concentration (20 and 200 U/mL collagenase type 4). (e) Encapsulated FITC-BSA released in proportion to hydrogel degradation with higher rates of molecule release corresponding with higher levels of MMP activity. (mean±SD, n=3 hydrogels per condition).

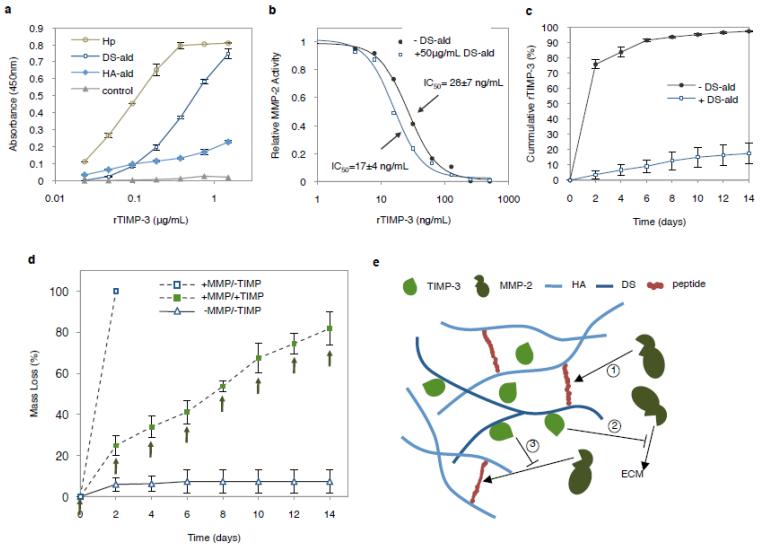

Figure 2. The non-covalent incorporation of rTIMP-3 into hydrogels and on-demand release in response to MMP activity

Release of encapsulated rTIMP-3 was controlled through incorporation of sulfate groups (in DS polymers) to bind rTIMP-3 via electrostatic interactions and MMP-cleavable crosslinks to release encapsulated rTIMP-3 as the hydrogel degrades in the presence of MMPs. (a) rTIMP-3 bound to polymer-coated wells and was detected with ELISA. rTIMP-3 bound to DS-ald with a greater capacity than HA-ald, and approached rTIMP-3 binding to heparin. (b) rTIMP-3 activity measured by its ability to inhibit a 4 nM rMMP-2 solution. rTIMP-3 binding to DS-ald did not significantly reduce rMMP-2 inhibition. (c) Passive release of rTIMP-3 (no MMP) encapsulated in 3.5 wt% ALD/HYD crosslinked hydrogels was drastically reduced by incorporation of sulfated DS-ald polymers into the hydrogels. (d) Hydrogels with (filled symbols) and without (open symbols) encapsulated rTIMP-3 (10 µg/50 µL gel) were incubated with (squares) or without (triangles) 20 nM rMMP-2. rMMP-2 was refreshed every two days to maintain enzyme activity (indicated by green arrows). Encapsulated rTIMP-3 attenuated MMP-2 mediated hydrogel degradation, confirming activity of rTIMP-3 across the 14-day study. (e) In this hydrogel system, rMMP-2 degrades the hydrogel crosslinks (1), liberating polysaccharide bound rTIMP-3, which inhibits local rMMP-2 activity (2), and attenuates further hydrogel degradation (3).

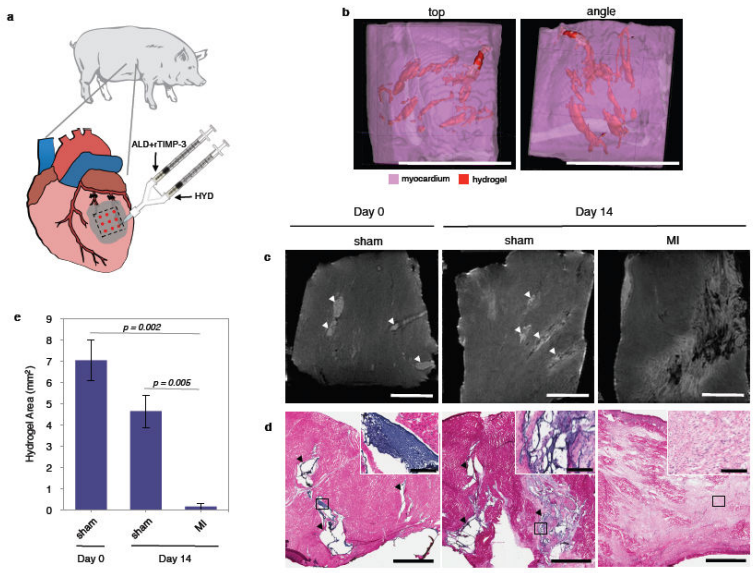

Figure 3. The visualization of injected hydrogel distribution and degradation within porcine myocardium

(a) A pig model of myocardial infarction (MI) was utilized to investigate the responsiveness of hydrogels post MI. Hydrogels (3.5 wt%) containing rTIMP-3 were injected into the myocardium at 9 equally spaced sites (100 μL per injection) within a 2 cm by 2 cm grid. Hydrogels were formed *in situ* by blending ALD and HYD modified polysaccharides immediately prior to entering the tissue using a dual barrel syringe. Hydrogels were injected into tissue with normal MMP activity (sham) and pathological MMP activity (experimental MI) and hydrogels were analyzed immediately after injection and after 14 days *in vivo*. Transmural myocardial explants of the injection grid were imaged with MRI, which allowed visualization of hydrogels within the myocardium. (b) Three-dimensional reconstruction of the MRI images using ITKsnap software shows pockets of hydrogel throughout the myocardium (scale bars = 2 cm). (c) Representative MRI images of injection grid tissue immediately following hydrogel injection and 14 days following injection in sham and MI animals (scale bars = 10 mm). Hydrogel pockets are still visible 14 days following injection in sham pigs but not in MI animals (d) Representative histological sections of injection grid tissue following hematoxylin and eosin staining. Pockets of hydrogels were visible in sham pigs 14 days following injection but not in MI animals (scale bars = 2 mm). Black arrows indicate regions of hydrogel identified by dark purple staining. Inset indicated by black box (scale bars = 200 μm). (e) Quantification of hydrogels within tissue across groups showed significantly less hydrogel in the myocardium from MI pigs compared to sham pigs after 0 and 14 days following injection (mean±SEM, n=3 pigs per group, pairwise t-test with Bonferroni correction).

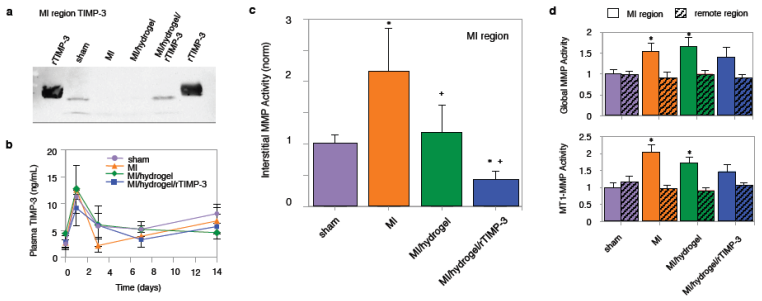

Figure 4. Hydrogel delivery of rTIMP-3 delivery alters the MMP/TIMP imbalance post MI

Hydrogels with and without encapsulated rTIMP-3 were injected immediately following experimental MI and myocardial MMP/TIMP levels were assessed 14 days post MI. (a) Hydrogel delivery of rTIMP-3 restored TIMP-3 levels within the MI region to normal, non-MI levels. (b) Blood samples revealed no significant increase in systemic TIMP-3 levels with hydrogel mediated rTIMP-3 delivery to the MI region. (c) Interstitial microdialysis of a fluorogenic MMP substrate into myocardium at 14 days post MI showed a significant increase in MMP activity within the MI region following MI induction. Injection of the MMP-cleavable hydrogels significantly inhibited MMP activity, and rTIMP-3 encapsulation further inhibited MMP activity. (d) Myocardial tissue extracts were harvested 14 days post MI and subjected to MMP activity assays using substrates for global MMP activity and membrane type-1 MMP (MT1-MMP) activity. A significant increase in both global MMP activity and MT1-MMP activity was observed following MI induction. This increase was abrogated with hydrogel/rTIMP-3 delivery. All values are mean±SEM; sham n=5, MI n=6, MI/hydrogel n=7, MI/hydrogel/rTIMP-3 n=7; pairwise t-test with Bonferroni correction; *p<0.05 vs. sham, +p<0.05 vs. MI, #p<0.05 vs. MI/hydrogel.

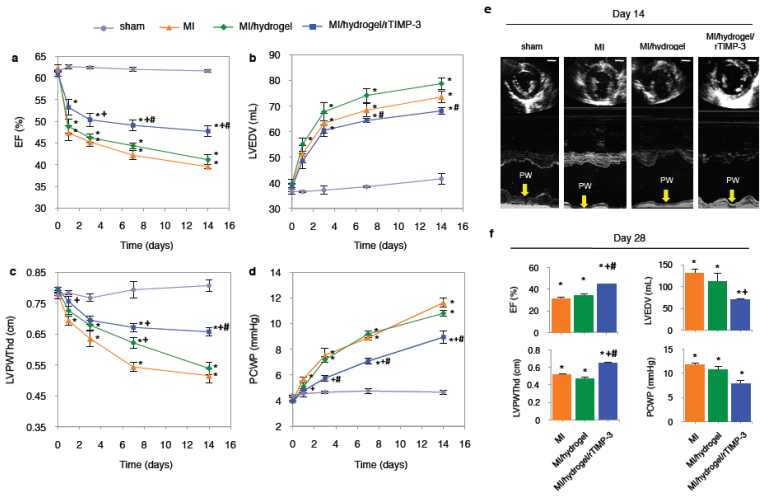

Figure 5. Hydrogel delivery of rTIMP-3 attenuates adverse LV remodeling and improves cardiac function post MI

Hydrogels with and without encapsulated rTIMP-3 were injected immediately following experimental MI and LV geometry and function was assessed with echocardiography. (a) MI induction caused a gradual decline in ejection fraction (EF) over 14 days which was significantly attenuated by hydrogel/rTIMP-3 delivery. (b) MI induction caused a gradual dilation of the LV end diastolic volume (LVEDV). Hydrogel/rTIMP-3 delivery significantly attenuated LVEDV compared to hydrogel delivery alone. (c) MI induction caused progressive thinning of the LV posterior wall thickness at diastole (LVPWThd) which was significantly attenuated by both hydrogel and hydrogel/rTIMP-3 injections at early timepoints, but only hydrogel/rTIMP-3 injections significantly attenuated wall thinning by day 14. (d) MI induction caused a steady increase in pulmonary capillary wedge pressure (PCWP) which was significantly attenuated by hydrogel/rTIMP-3 delivery. (e) Representative short axis views (top) and m-mode targeted images (bottom) for each treatment group 14-days post MI (scale bars = 1 cm). The posterior wall (PW) at the site of the infarct induction is shown by the arrows. Significant chamber dilation and wall thinning occurred following MI-consistent with the adverse remodeling process, which was unaffected by hydrogel injection only. However, the degree of LV dilation and wall thinning was attenuated in the hydrogel/rTIMP-3 group. (f) Hydrogel/rTIMP-3 injections continued to show a therapeutic benefit 28 days following MI induction, a critical time in the progression of adverse LV remodeling. All values are mean±SEM; (a-d) sham n=5, MI n=6, MI/hydrogel n=7, MI/hydrogel/rTIMP-3 n=7; (f) n=3 for all groups; pairwise t-test with Bonferroni correction; *p<0.05 vs. sham, +p<0.05 vs. MI, #p<0.05 vs. MI/hydrogel.